Computer Modeling in Engineering & Sciences

Tech Science Press

DOI: 10.32604/cmes.2023.030872

ARTICLE

Outage Analysis of Optimal UAV Cooperation with IRS via Energy Harvesting Enhancement Assisted Computational Offloading

Baofeng Ji[1,2,3,*], Ying Wang[1,2,3], Weixing Wang[1], Shahid Mumtaz[4] and Charalampos Tsimenidis[4]

[1]School of Information Engineering, Henan University of Science and Technology, Luoyang, 471000, China

[2]Research and Innovation Center of Intelligent System, Longmen Laboratory, Luoyang, 471000, China

[3]State Key Laboratory of Complex Electromagnetic Environment Effects on Electronics and Information System (CEMEE), Luoyang, 471000, China

[4]Sustainable Digital Communications and Energy Systems (DIGCOM) Group, Nottingham Trent University, Nottingham, UK

*Corresponding Author: Baofeng Ji. Email: baofengjihkd@163.com

Received: 28 April 2023 Accepted: 06 July 2023 Published: 17 November 2023

ABSTRACT

The utilization of mobile edge computing (MEC) for unmanned aerial vehicle (UAV) communication presents a viable solution for achieving high reliability and low latency communication. This study explores the potential of employing intelligent reflective surfaces (IRS) and UAVs as relay nodes to efficiently offload user computing tasks to the MEC server system model. Specifically, the user node accesses the primary user spectrum, while adhering to the constraint of satisfying the primary user peak interference power. Furthermore, the UAV acquires energy without interrupting the primary user's regular communication by employing two energy harvesting schemes, namely time switching (TS) and power splitting (PS). The selection of the optimal UAV is based on the maximization of the instantaneous signal-to-noise ratio. Subsequently, the analytical expression for the outage probability of the system in Rayleigh channels is derived and analyzed. The study investigates the impact of various system parameters, including the number of UAVs, peak interference power, TS, and PS factors, on the system's outage performance through simulation. The proposed system is also compared to two conventional benchmark schemes: the optimal UAV link transmission and the IRS link transmission. The simulation results validate the theoretical derivation and demonstrate the superiority of the proposed scheme over the benchmark schemes.

KEYWORDS

Unmanned aerial vehicle (UAV); intelligent reflective surface (IRS); energy harvesting; computational offloading; outage probability

1 Introduction

The rapid advancement of emerging technologies, including Artificial Intelligence (AI), Internet of Things (IoT), and Internet of Everything (IoE), has led to an exponential increase in wireless connectivity. This growth presents a significant challenge for data-centric automation systems [1]. This challenge necessitates the deployment of a considerable number of base stations and wireless terminals to support the increasing demand for mobile services and large-scale wireless connections. However,

This work is licensed under a Creative Commons Attribution 4.0 International License, which permits unrestricted use, distribution, and reproduction in any medium, provided the original work is properly cited.

this trend also poses a challenge for future wireless communication systems, as they must contend with highly complex networks, escalating hardware costs, and a surge in energy consumption. To address this pressing issue, there is an immediate need for a novel solution that achieves a balance between system performance and energy consumption costs [2,3].

In recent years, Unmanned Aerial Vehicles (UAVs) have garnered significant interest due to their high mobility and flexible deployment capabilities. Their flexibility, portability, powerful line-of-sight communication links, and low-cost, changeable use have made them increasingly popular in both research and commercial applications. Their essential features enable a wide range of civilian services, including transport and industrial monitoring, agriculture, forest fire management, and wireless services. However, the surge in data volume of wireless networks poses a significant challenge to the computing power demand of equipment. The current terminals are generally limited in computing resources and battery capacity. Mobile edge computing (MEC) is a novel computing technology that enables the transfer of computing power from the cloud to the edge of the network, thereby enhancing the efficiency of data processing and transmission. By integrating wireless networks and technologies, and deploying computing and storage resources at the edge of the network closer to mobile devices or sensors, MEC significantly alleviates the pressure on the network and data center, enhances server response ability, protects privacy data, reduces the risk of data uploading and sharing in the cloud, and focuses on real-time, short-cycle data analysis. MEC meets the key requirements of IoT digitization in agile connection, business implementation, data optimization, application intelligence, security, and privacy protection. It is anticipated that the integration of MEC and UAVs will provide robust support for embracing the forthcoming era of the Internet of Drones (IOD).

In effect, there is already a substantial body of literature exploring MEC enabled drone solutions. Reference [4] introduced three MEC architectures that support UAVs, which improve communication performance and reduce execution latency. A MEC wireless power supply system for UAVs was developed by [5], and the computational rate maximization problem in the UAVs MEC wireless power supply system was solved. The problem was constrained by the causal constraints of energy acquisition and UAV speed. Reference [6] designed a UAV-assisted MEC computing offloading scheme based on deep reinforcement learning to minimize the total cost, which is the weighted sum of delay, energy consumption, and bandwidth costs. Reference [7] proposed a resource pricing and trading scheme based on Stackelberg dynamic game to optimize the allocation of MEC resources, and applied blockchain technology to record the entire resource trading process to protect security and privacy. Reference [8] put forth two offloading schemes for enabling MEC networks in multiple UAVs. Their optimization goal is to minimize the global computing time and energy consumption of all drones, respectively. Reference [9] advanced four representative architectures of MEC systems based on UAVs, and by adopting software defined networks, the scalability and controllability of the network are improved.

The design of contemporary wireless communication systems has placed significant emphasis on spectrum and energy efficiency. In this regard, Intelligent Reflective Surface (IRS) has emerged as a promising green communication technology. IRS is passive, low-cost, and easily deployable, and has garnered extensive attention [10]. As a promising technology for future wireless networks, it supports energy-saving and cost-effective communication, and is considered one of the most promising 6G wireless communication technologies [11]. Through the use of low-cost passive components that exploit time-varying environments, IRS dynamically adjusts the phase shifts of reflected signals to modify the wireless propagation environment, resulting in high passive beamforming gains and improved efficiency of wireless power transmission [12]. IRS technology operates in full-duplex mode and consumes low power, making it a promising solution for enhancing both energy efficiency and

spectral efficiency. Moreover, several studies have demonstrated the advantages of IRS technology by comparing it with other technologies. In one study [13], a comparison was made between the performance of IRS and decoding and forwarding (DF) relays, and it was concluded that even static relays with relatively low degrees of freedom require very high rates and/or larger IRS to outperform DF relays. In another study [14], the performance of mobile relays and IRS was compared, and it was found that mobile relays achieved a higher communication average signal-to-noise ratio than IRS, primarily due to the greater degree of freedom of motion of mobile relays. However, IRS still possesses certain inherent advantages over relays, such as lower cost and higher energy efficiency. Specifically, the work in [11] demonstrates that a proposed resource allocation method based on IRS can achieve up to 300% higher energy efficiency than traditional amplification and forwarding (AF) relay-based communication systems by appropriately designing the phase shifts of RIS applications. Additionally, in [15], it was suggested that IRS can be utilized to actively reprogram the communication environment, and its advantages in terms of coverage, energy conservation, and security are discussed.

As further research is conducted, the potential applications of IRS-assisted wireless networks in various scenarios and technologies continue to unfold. These scenarios include IRS-assisted Multiple Input Multiple Output (MIMO) [16–18], IRS-assisted large-scale MIMO [19], IRS-assisted mobile edge computing [20], IRS-assisted Unmanned Aerial Vehicle (UAV) communication [21,22], IRS-assisted physical layer security [23–26], robust beamforming design in IRS-assisted Multiple Input Single Output (MISO) communication [27], IRS-assisted Simultaneous Wireless Information and Power Transmission (SWIPT) [28–35], and IRS-enhanced non-orthogonal multiple access transmissions [36–38].

In light of this, this study considers a system model where UAVs and IRS assist users in offloading computing to edge servers, as presented in the third application scenario in [4]. To address the issue of energy consumption, the study also explores the use of cognitive radio network (CRN) based energy harvesting technology, which can provide more efficient, stable, and dependable communication services.

The contributions of this article are as follows:

Firstly, this paper proposed system model considers using IRS and UAV as relay nodes to effectively offload user computing tasks to the MEC server. In order to further alleviate the resource constraints faced by future wireless networks. The UAV in our model is energy harvesting enhanced.

Secondly, the computational offloading outage probability of the proposed model under Rayleigh channel is constructed and deduced. The correctness of the theoretical derivation is proved by the consistency between the theory and simulation. Additionally, a comparison is made with the computational offloading outage performance of traditional systems relying solely on IRS or only optimal relay links. The results clearly demonstrate that the proposed optimal relay cooperative IRS system exhibits a lower computational offloading outage probability, i.e., a higher computational offloading success rate.

This paper is organized as follows. Section 2 outlines the system model for the optimal UAV cooperative IRS to assist users in offloading computing to edge servers and provides a detailed description of the information transmission process. In Section 3, an analysis and derivation of the outage probability for the proposed model in Rayleigh channel is presented. Section 4 offers a comprehensive set of numerical evaluation results. Finally, Section 5 offers a summary of the findings.

2 System Model

This section introduces the system model proposed in this article and describes the information transmission process of the model.

2.1 System Model Description

As shown in Fig. 1, this paper considers the system model of the optimal UAV cooperative IRS offload user computing tasks to the MEC server that utilizes CRN energy harvesting. The system architecture is illustrated in Fig. 1, which consists of a primary user node P and a cognitive user node within the cognitive network S, K DF UAVs, a MEC server D and IRS equipped with N signal reflection elements. In this model, user S generate compute-intensive tasks. Because user have limited battery capacity and computing power and cannot handle compute-intensive and delay-sensitive tasks. Although UAV has more computing power than user, considering the inconsistencies and instability of energy harvesting, this paper chooses to offload computing tasks to edge servers with significantly better processing power than UAV. It is assumed in this paper that all nodes in the system are equipped with a single antenna. The UAV node also features an energy harvesting function, and two energy harvesting schemes, time switching (TS) and power splitting (PS), are adopted. These schemes are implemented to ensure that energy is not taken away from the primary user's communication. Instead, the energy is utilized for the UAV node to offload computing tasks to the MEC server. To address the communication challenges resulting from blocked line-of-sight link between the user and the MEC server, IRS is deployed on the exterior walls of tall buildings to dynamically adjust signal phase and intelligently reflect signals towards the intended recipient user. Moreover, given the presence of numerous UAVs in the high altitude platform, an optimal UAV R_k $(1 \leq k \leq K)$ is selected to support the communication process.

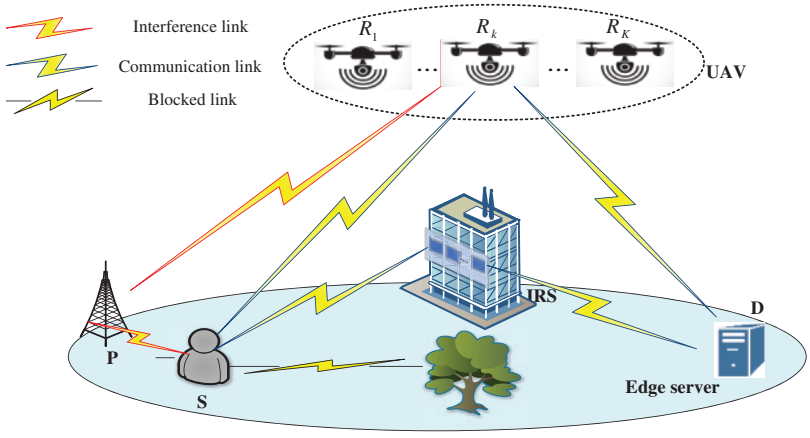

Figure 1: System model

The communication process between the user and the MEC server is predicated on the assumption that the signal is transmitted at fixed time intervals that are equally divided into two time slots. In the first time slot, the signal transmission link is established as $S \rightarrow R_k$, $R_k \rightarrow P$, $S \rightarrow P$, $S \rightarrow IRS$. Specifically, the user broadcasts the signal to both the UAV and the IRS with power P_S, subject to the constraint that the peak interference power I_P of the primary user is not exceeded. The UAV node endeavors to decode the received signal and forward it to the MEC server.

In the second time slot, the signal transmission link is established as $R_k \rightarrow D$, $IRS \rightarrow D$. The selection of the optimal UAV from the available UAV nodes is determined based on the maximization of the instantaneous signal-to-noise ratio at the MEC server [39,40]. The optimal UAV then decodes the signal and forwards it to the MEC server, utilizing the energy harvested at the UAV as transmission power. Furthermore, the IRS adjusts its phase to reflect the signal towards the intended recipient.

In the TS energy harvesting scheme, signal transmission time is bifurcated into two components. Throughout the entire signal transmission time T, $\rho\,(0 \leq \rho \leq 1)$ represents the time conversion coefficient. The first part ρT represents the duration expended by the UAV for energy harvesting, while the second part $(1-\rho)\,T$ indicates the time necessitated for the signal transmission from the user node, to the MEC server. Herein, the time mandated for signal transmission from the user node to the IRS and UAV is denoted by $(1-\rho)\,T/2$, while the time during which the signal is conveyed from the IRS to the MEC server and concurrently from the optimal UAV node to the MEC server is represented by $(1-\rho)\,T/2$.

In the PS energy harvesting scheme, power is apportioned into two components. η denotes a power division factor, ηP_S signifies the power utilized by the UAV node for energy harvesting, and $(1-\eta)\,P_S$ represents the power employed by the user node for information transmission. Correspondingly, the time designated for the initial and secondary time slots is $T/2$, respectively.

In this paper, it is postulated that all transmission channels adhere to independent and identically distributed Rayleigh fading channels with an average channel gain of Ω_u. The noise at each receiving node n_u is modeled as additive white Gaussian noise (AWGN) with a zero mean value and a variance of ${\sigma_u}^2$.

2.2 Information Transmission Process

In the first time slot, the user node sends signals to the UAV nodes and the IRS under the constraint of the peak interference power I_p of the primary user. At this time, the transmission power of the user node S is

$$P_I = \frac{I_P}{\left\|h_{sp}\right\|^2} \tag{1}$$

where, I_P represents the peak interference power, h_{sp} represents the channel parameter from the cognitive node to the primary user node, and $\left\|h_{sp}\right\|^2$ represents the channel gain of the link.

Under the TS and PS energy harvesting schemes, the power used by the user node to transmit signals is given as

$$TS\colon\ P_S = P_I \tag{2}$$

$$PS\colon\ P_S = (1-\eta)\,P_I \tag{3}$$

and the signals received by the kth $(1 \leq k \leq K)$ UAV are expressed as

$$y_{r_k} = \sqrt{P_S} h_{sr_k} + n_{sr_k} \tag{4}$$

where, h_{sr_k} is the channel parameter representing the user node to the kth relay, and n_{sr_k} is AWGN.

The channel capacity of the *kth* UAV is expressed as

$$C_{SR_k} = \frac{1}{2}\log_2\left(1+\gamma_{sr_k}\right) = \frac{1}{2}\log_2\left(1+\frac{P_S\left\|h_{sr_k}\right\|^2}{{\sigma_{sr_k}}^2}\right) = \begin{cases} TS\dfrac{1}{2}\log_2\left(1+\dfrac{P_I\left\|h_{sr_k}\right\|^2}{{\sigma_{sr_k}}^2}\right) \\ PS\dfrac{1}{2}\log_2\left(1+\dfrac{(1-\eta)\,P_I\left\|h_{sr_k}\right\|^2}{{\sigma_{sr_k}}^2}\right) \end{cases} \tag{5}$$

where, γ_{sr_k} is the signal to noise ratio at the *kth* UAV.

The UAV node functions in DF mode. When the capacity of the UAV received signal C_{SR_k} surpasses a specified threshold value R_{th} ($R_{th} \geq 0$), the UAV successfully decodes the received signal and forwards it. Conversely, if the capacity of the UAV received signal C_{SR_k} is less than the threshold value R_{th}, the UAV fails to decode the signal, and the UAV node ceases transmission. Therefore, the probability that the secondary UAV cannot successfully decode the signal is

$$P_{fail}^k = \Pr\left(C_{SR_k} \leq R_{th}\right) = \begin{cases} TS\colon\ \Pr\left(\dfrac{\left\|h_{sr_k}\right\|^2}{\left\|h_{sp}\right\|} \leq \alpha_1\right) \\ PS\colon\ \Pr\left(\dfrac{\left\|h_{sr_k}\right\|^2}{\left\|h_{sp}\right\|} \leq \alpha_2\right) \end{cases} \tag{6}$$

where, $\alpha_1 = \dfrac{\left(2^{2R_{th}}-1\right){\sigma_{sr_k}}^2}{I_p}$, $\alpha_2 = \dfrac{\left(2^{2R_{th}}-1\right){\sigma_{sr_k}}^2}{(1-\eta)\,I_p}$. Furthermore, we define Φ as the set of UAVs that have successfully decoded and forwarded received signals in K relays. When the number of relays is K, the subset of Φ has a total of 2^K. At this time, the sample space can be written as $\Phi = \{\varnothing, \Phi_2, \Phi_3, \ldots, \Phi_k, \ldots, \Phi_{2^K}\}$, with Φ_k representing the *kth* subset of the decoding set Φ, where, the number of UAVs containing successful decoding is $|\Phi_k| = L$, $(0 \leq L \leq K)$.

Assuming that the channel state information of all links is available, the aforementioned optimal UAV selection is based on the strategy of maximizing the signal-to-noise ratio. In other words, it relies on the instantaneous signal-to-noise ratio maximization at the legitimate user node D. This involves selecting the optimal node to forward information from the decoded UAV set Φ as expressed below:

$$k^* = \underset{k\subset\Phi}{argmax}\left\|h_{r_k d}\right\|^2. \tag{7}$$

Next, we calculate the energy harvested at the *kth* UAV under the TS and PS energy harvesting schemes as

$$TS\colon E_{R_k} = \xi P_I\left\|h_{sr_k}\right\|^2\rho T \tag{8}$$

$$PS\colon E_{R_k} = \xi\eta P_I\left\|h_{sr_k}\right\|^2\frac{T}{2} \tag{9}$$

where, ξ represents the energy conversion efficiency.

At this point, the energy harvested at the UAV will be used to forward the signal, and its power is expressed as

$$TS\colon P_{R_k} = \min_{k\subset\Phi}\left(\frac{E_{R_k}}{(1-\rho)\frac{T}{2}}, \frac{I_p}{\left\|h_{r_{kp}}\right\|^2}\right) \tag{10}$$

$$PS\colon P_{R_k} = \min_{k\subset\Phi}\left(\frac{E_{R_k}}{\frac{T}{2}}, \frac{I_p}{\left\|h_{r_{kp}}\right\|^2}\right) \tag{11}$$

where, $h_{r_{kp}}$ is a channel parameter representing the channel from the kth UAV node to the primary user node. Similarly, at this time, the transmission power at the kth UAV must also meet the constraints of the peak interference power I_P of the primary user.

At this point, the signals received by the MEC server from the optimal UAVk^* and IRS can be represented as

$$y_{k^*} = \sqrt{P_{k^*}}h_{k^*d}x + n_D \tag{12}$$

$$y_{IRS} = \sqrt{P_S}h_{id}{}^H\Theta h_{si}x + n_I \tag{13}$$

where, h_{k^*d} is the channel parameter representing the optimal UAV k^* to the MEC server D, h_{si} is the channel parameter representing the source node S to the IRS, h_{id} is the channel parameter representing the IRS to the MEC server D, $\Theta = diag\{\beta_1 e^{j\varphi_1}, \beta_2 e^{j\varphi_2}, \cdots, \beta_N e^{j\varphi_N}\}$ represents the IRS phase shift; herein, $\varphi_n \in [0, 2\pi)$, $1 \le n \le N$, and assuming that the IRS can only change the phase of the incident signal, the reflection coefficient of each reflection element meets the following constraints: $\beta_n = 1$.

Since all links in the model in this paper adopt Rayleigh fading channels, all channel gains $\|h_u\|^2$ are subject to Rayleigh distribution. The probability density function (PDF) and cumulative distribution function (CDF) are respectively represented by the following formulas:

$$f_{h_U}(x) = \frac{1}{\Omega_u}e^{-\frac{x}{\Omega u}} = \lambda_u e^{-\lambda_u x} \tag{14}$$

$$F_{h_U}(x) = 1 - e^{-\frac{x}{\Omega u}} = 1 - e^{-\lambda_u x} \tag{15}$$

where, $\Omega_u = E\left[\|h_u\|^2\right]$ represents the expectation of channel gain, $\lambda_u = \dfrac{1}{\Omega_u}$.

Letting $h_S = \dfrac{h_{SP}}{h_{SR_K}} = \dfrac{\left\|h_{sp}\right\|^2}{\left\|h_{sr_k}\right\|^2}$, where $h_{sr_k} \in h_{sk}$, the PDF of h_S can be represented by the following formula:

$$\begin{aligned} f_{h_S}(z) &= \int_0^\infty y f_{h_{SP}}(zy) f_{h_{SR_K}}(y)\, dy \\ &= Q_1 \frac{1}{\left(z\lambda_{sp} + \lambda_{sk}\right)^2} \end{aligned} \tag{16}$$

where $Q_1 = \lambda_{sp}\lambda_{sk}$.

3 Outage Probability Performance Analysis

This section concerns the derivation and analysis of a closed-form expression for the outage probability of the optimal UAV cooperative IRS offload user computing tasks to the MEC server system model.

The outage probability of a system is a measure of its link capacity, representing the probability of the link being unable to meet the minimum required transmission rate γ_{th}. Applying the total probability formula, the outage probability of the optimal UAV cooperative IRS system can be formulated as follows:

$$\begin{aligned} P_{out} &= \Pr\left(C_R \le \gamma_{th}\right)\Pr\left(C_{IRS} \le \gamma_{th}\right) \\ &= \left(\Pr\left(\Phi = \varnothing\right) + \sum_{n=1}^{2^N-1}\Pr\left(C_R \le \gamma_{th}, \Phi = |\Phi_n|\right)\right)\Pr\left(C_{IRS} \le \gamma_{th}\right) \\ &= \underbrace{\left(\Pr\left(\Phi = \varnothing\right) + \sum_{n=1}^{2^N-1}\underbrace{\Pr\left(\Phi = |\Phi_n|\right)}_{\mathrm{I}_1}\underbrace{\Pr\left(C_R \le \gamma_{th} \,|\Phi = |\Phi_n|\right)}_{\mathrm{I}_2}\right)}_{A}\underbrace{\Pr\left(C_{IRS} \le \gamma_{th}\right)}_{B} \end{aligned} \tag{17}$$

where, C_R and C_{IRS} represent the capacity of the MEC server to receive from the UAV link and the IRS link, respectively. Moreover, A and B represent the outage probability of the UAV link and the IRS link, respectively. Only when both links are interrupted simultaneously will the entire system be interrupted.

3.1 Optimal UAV Link Outage Probability

$\Pr\left(\Phi = \varnothing\right)$ indicates the probability that all UAVs fail to decode the signal successfully in the first time slot. Using the binomial expansion formula $\left(\frac{K_1}{I_P U_1}y + \beta_1 z\right)^q = \sum_{s=0}^{q}\binom{q}{s}\left(\beta_1 z\right)^s\left(\frac{K_1}{I_P U_1}y\right)^{q-s}$ and bringing $f_{SP}\left(x\right)$ in the expression, it can be obtained that

$$\begin{aligned} \Pr\left(\Phi = \varnothing\right) &= \prod_{1\le k\le N}\Pr\left(\frac{\left\|h_{sr_k}\right\|^2}{\left\|h_{sp}\right\|^2} \le \alpha\right) = \int_0^\infty\left[F_{h_{SR_K}}\left(\alpha x\right)\right]^N f_{h_{SP}}\left(x\right)dx \\ &= \sum_{r=0}^{N}\binom{N}{r}\left(-1\right)^r\lambda_{sp}\frac{1}{r\alpha\lambda_{sk}+\lambda_{sp}} \end{aligned} \tag{18}$$

$\Pr\left(\Phi = |\Phi_n|\right)$ indicates the probability that the number of successfully decoded relays in the UAV set is L. Similarly, using the binomial expansion formula and incorporating $f_{SP}\left(x\right)$ into the expression, it can be calculated as follows:

$$\begin{aligned} \mathrm{I}_1 &= \Pr\left(\Phi = |\Phi_n|\right) = \int_0^\infty\prod_{k\subset\Phi_n}\Pr\left(\left\|h_{sr_k}\right\|^2 > \alpha x\right)\times\prod_{v\subset\overline{\Phi}_n}\Pr\left(\left\|h_{sr_v}\right\|^2 \le \alpha x\right)f_{h_{SP}}\left(x\right)dx \\ &= \int_0^\infty\binom{N}{L}\sum_{S=0}^{L}\binom{L}{S}\left(-1\right)^S\left(F_{h_{SR_k}}\left(\alpha x\right)\right)^{S+N-L}f_{h_{SP}}\left(x\right)dx \\ &= \sum_{S=0}^{L}\sum_{d=0}^{S+N-L}\binom{N}{L}\binom{L}{S}\binom{S+N-L}{d}\frac{\lambda_{sp}\left(-1\right)^{S+d}}{\alpha d\left(\lambda_{sk}+\lambda_{sp}\right)} \end{aligned} \tag{19}$$

$\Pr(C_R \le R_{th} | \Phi = |\Phi_n|)$ indicates the probability that the capacity will be less than when the UAV successfully decodes the information. The calculation process is as follows:

$$I_2 = \Pr(C_R \le \gamma_{th} | \Phi = |\Phi_n|) = \begin{cases} TS: \prod\limits_{k \subset |\Phi_n|} \left\{ \begin{array}{l} \underbrace{\Pr\left(h_{K^*D} \le \dfrac{K}{U_1} h_S, h_S \ge h_{K^*P} U_1\right)}_{W_1} \\ + \underbrace{\Pr\left(h_{K^*D} \le K h_{K^*P}, U_1 h_{K^*P} > h_S\right)}_{W_2} \end{array} \right\} \\ PS: \prod\limits_{k \subset |\Phi_n|} \left\{ \begin{array}{l} \underbrace{\Pr\left(h_{K^*D} \le \dfrac{K}{U_2} h_S, h_S \ge h_{K^*P} U_2\right)}_{W_3} \\ + \underbrace{\Pr\left(h_{K^*D} \le K h_{K^*P}, U_2 h_{K^*P} > h_S\right)}_{W_4} \end{array} \right\} \end{cases} \tag{20}$$

where, $U_1 = \dfrac{2\xi\rho}{1-\rho}$, $K = \dfrac{\sigma_D^2(\beta-1)}{I_p}$, $\beta = 2^{2\gamma_{th}}$. Using binomial expansion formulas, i.e., $\int_0^\infty \dfrac{x^{\alpha-1}}{(x+z)^\rho} e^{-px} dx = \gamma(\alpha) z^{\alpha-\rho} \psi(\alpha, \alpha+1-\rho, pz)$, $\mathrm{Re}\alpha, \mathrm{Re}\rho > 0; \{\arg z\} < \pi$, and $\int_0^\infty x^{v-1} e^{-ux} dx = \dfrac{\Gamma(v)}{u^v}$, ($\mathrm{Re}u > 0$, $\mathrm{Re}v > 0$), we can exchange the integration order. Thus, the calculation process of W_1 is as follows:

$$\begin{aligned} W_1 &= \Pr\left(h_{K^*D} \le \frac{K}{U_1} h_S, h_S \ge h_{K^*P} U_1\right) \\ &= \int_0^\infty \int_{U_1 x}^\infty F_{K*D}\left(\frac{K}{U_1} y\right) f_{h_S}(y)\, dy f_{h_{K^*P}}(x)\, dx \\ &= Q_1 \int_0^\infty \frac{1}{\left(y\lambda_{sp} + \lambda_{sk}\right)^2} - e^{-\frac{\lambda_{k^*p}}{U_1} y} \frac{1}{\left(y\lambda_{sp} + \lambda_{sk}\right)^2} \\ &\quad - e^{-\frac{K\lambda_{k^*d}}{U_1} y} \frac{1}{\left(y\lambda_{sp} + \lambda_{sk}\right)^2} + e^{-\left(\frac{K\lambda_{k^*d}}{U_1} + \frac{\lambda_{k^*p}}{U_1}\right) y} \frac{1}{\left(y\lambda_{sp} + \lambda_{sk}\right)^2} dy \\ &= 1 - \psi\left(1, 0, \frac{\lambda_{k*p}\lambda_{sk}}{U_1\lambda_{sp}}\right) - \psi\left(1, 0, \frac{K\lambda_{k*d}\lambda_{sk}}{U_1\lambda_{sp}}\right) + \psi\left(1, 0, \frac{K\lambda_{k*d}\lambda_{sk} + \lambda_{k*p}\lambda_{sk}}{U_1\lambda_{sp}}\right) \end{aligned} \tag{21}$$

where, $\psi(a, b, c)$ is the confluent hypergeometric function, and $\psi(1, 0, 0) = 1$.

Similarly, the calculation process of W_2 is as follows:

$$\begin{aligned} W_2 &= \Pr\left(h_{K^*D} \le K h_{K^*P}, U_1 h_{K^*P} > h_S\right) \\ &= \int_0^{\infty} \int_{\frac{U_1}{x}}^{\infty} F_{h_{K^*D}}(Ky) f_{h_{K^*P}}(y)\, dy f_{h_S}(x)\, dx \\ &= -1 + \frac{1}{K+1} + \psi\left(1, 0, \frac{\lambda_{k*p}\lambda_{sk}}{U_1\lambda_{sp}}\right) - \frac{\lambda_{k*p}}{\left(K\lambda_{k*d} + \lambda_{k*p}\right)} \psi\left(1, 0, \frac{K\lambda_{k*d}\lambda_{sk} + \lambda_{k*p}\lambda_{sk}}{U_1\lambda_{sp}}\right) \end{aligned} \tag{22}$$

W_3 and W_4 can be calculated by following similar approaches.

The precise closed expression of the optimal UAV link outage probability is given as

$$\Pr\left(C_R \le \gamma_{th}\right) = \sum_{L=0}^{N} I_1 \left(I_2\right)^L \tag{23}$$

3.2 IRS Link Outage Probability

The CDF of the signal-to-noise ratio of the IRS link under Rayleigh fading channels has been explicitly provided in literature [41] as

$$\Pr\left(C_{IRS} \le \gamma_{th}\right) = F\left(\gamma_{th}\right) \approx \frac{1}{\Gamma\left(k_w\right)\Gamma\left(m_w\right)} G_{1,3}^{2,1}\left[\tilde{\Xi}\gamma_{th}\big|_{k_w, m_w, 0}^{1}\right] \tag{24}$$

where, $\tilde{\Xi} = \sqrt{k_w m_w / \left(\overline{\gamma}_1 \Omega_w\right)}$, $k_w = \dfrac{-b + \sqrt{b^2 - 4ac}}{2a}$ and $m_w = \dfrac{-b - \sqrt{b^2 - 4ac}}{2a}$ are shaping parameters, and the values of a, b and c are defined in the paper [42]. $\overline{\gamma}_1$ represents the average signal-to-noise ratio.

In summary, the outage probability of the proposed system model in the calculation primarily encompasses determining the optimal UAV link outage probability and IRS link outage probability. The specific algorithmic flow is illustrated in Table 1. Initially, UAV link transmission entails the user node transmitting signals to multiple UAV nodes with power P_S under the constraint of peak interference power I_P. The UAV node ascertains whether K relays have successfully decoded the information and incorporates the successfully decoded relays into the set Φ. Subsequently, the optimal UAV selection strategy based on the maximum signal-to-noise ratio of the destination node is chosen. When the UAV node satisfies the constraint of the primary user's peak interference power, it forwards the signal to the MEC server with power $P_{R_{k^*}}$. Subsequently, it compares the outage capacity threshold γ_{th} of the MEC server with the capacity of the optimal UAV link to determine link interruption. Due to the passive reflection characteristics of IRS, the IRS link interruption implies that the capacity of the target IRS link to receive signals is smaller than the outage capacity threshold γ_{th}. It is crucial to note that when the IRS link and the optimal UAV link are interrupted simultaneously, the entire system is disrupted.

Table 1: Energy harvesting enhanced optimal UAV cooperative IRS outage probability algorithm

Algorithm 1 The outage probability of energy harvesting enhanced optimal UAV cooperative IRS

Input: N, the number of IRS elements
K, the number of relay
L, the number of successful decoding UAV
I_P, peak interference power
P_S, the power used by the source node to send information
P_{R_k}, the power of UAV
Output: P_{out}, outage probability
Initialize $N = 3$, $K = 3$, $L = 0$, $\sigma_u^2 = 1$, $\Omega_u = 1$, $\rho = 0.5$, $\eta = 0.5$, $P_r(C_R \leq \gamma_{th}) = 0$
for $I_P = 20$dB, I_P++, **do**
  for $k = 1$, k++, $k \leq K$ **do**
    Calculate P_S under TS and PS energy harvesting schemes using (2) and (3)
    Calculate the channel capacity of each UAV and check whether the information is successfully decoded
      if $C_{SR_k}(k) \geq R_{th}$
        Calculate P_{R_k} using (10) and (11)
      else
        $P_{R_k} \leftarrow 0$
    end if
    for $L = 0$, $L \leq K$, L++ **do**
      The optimal UAV is selected from the set Φ based on instantaneous signal-to-noise ratio maximization
      $P_{R_{k^*}} \leftarrow P_{R_k}(L)$
    end for
  Calculate the channel capacity of the IRS link and the optimal UAV link at the MEC server
  end for
$P_r(C_R \leq \gamma_{th}) = P_r(C_R \leq \gamma_{th}) + sum(C_R \leq \gamma_{th})$
$P_{out} = P_r(C_R \leq \gamma_{th}) \cdot P_r(C_{IRS} \leq \gamma_{th})$
end for
return P_{out}

4 Simulation and Result Analysis

This study employs Monte Carlo simulation to validate the accuracy of the proposed scheme and theory in deriving the closed expression and examines the effect of various parameters on its outage performance. Additionally, a comparison is made with the outage performance of traditional systems that rely solely on IRS or only optimal UAV links. The results clearly demonstrate that the proposed optimal UAV cooperative IRS system exhibits a lower outage probability, i.e., higher stability and reliability.

To facilitate analysis and simulation, it is assumed that parameters related to network size are set to a smaller value, and the initial values of each parameter are set to $N = 3$ and $K = 3$. During the simulation process, the UAV decoding threshold is $R_{th} = 0.5$, the system outage threshold is set to $\gamma_{th} = 0.5$, the time conversion factor of TS scheme is $\rho = 0.5$, PS energy conversion factor $\eta = 0.5$, energy conversion coefficient $\xi = 1$, and AWGN variance $\sigma_u^2 = 1$. The channels are all Rayleigh fading channels, and it is assumed that the channel parameters are identical, with an average channel power gain $\Omega_u = 1$. The simulation results reveal that the derivation results of the proposed scheme in this study align well with the Monte Carlo simulation results, which substantiates the accuracy of the derivation and analysis in this study and the feasibility of the scheme.

Fig. 2 simulates the change curve of outage probability with the primary user's peak interference power I_p under different UAV decoding thresholds R_{th} and various energy harvesting schemes. As I_p gradually increases, the system outage probability progressively diminishes and approaches zero, that is, the probability of successfully offloading user computing tasks to the MEC server increases. This is because the I_p increase signifies that the user and UAV nodes can transmit signals with greater power without disrupting the primary user's normal communication. As the UAV decoding threshold R_{th} continues to rise, the system outage probability enlarges and the probability of computing offloading process interruption increases. And under identical conditions, the system performance utilizing TS energy harvesting scheme is superior to that of the PS energy harvesting scheme.

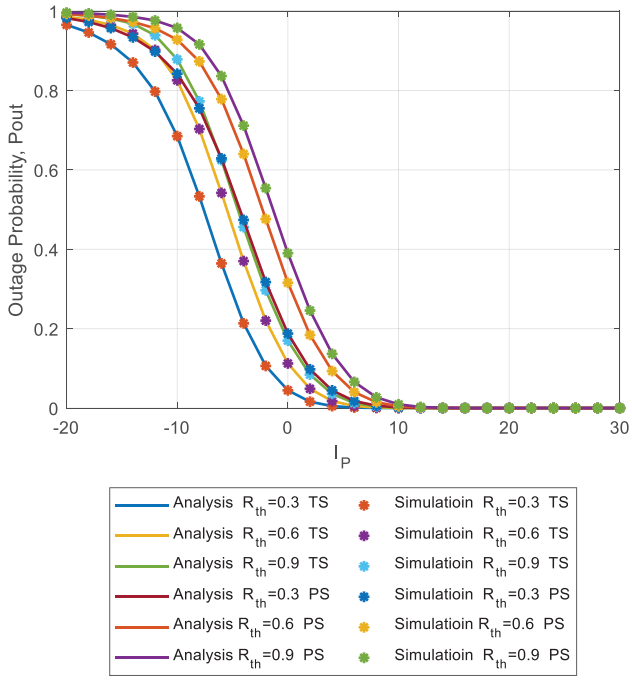

Figure 2: The curves of outage probability with different R_{th} and energy harvesting scheme

Fig. 3 simulates the change curve of outage probability with UAV decoding threshold R_{th} under different primary user peak interference power I_P and various energy harvesting schemes. Simulation results demonstrate that with the increase of the UAV decoding threshold R_{th}, the probability of successful UAV decoding decreases, resulting in an increase in the system computation offloading outage probability. Under the same energy harvesting scheme and the same UAV decoding threshold

R_{th}, a larger signal-to-noise ratio can compensate for the performance loss under adverse decoding conditions.

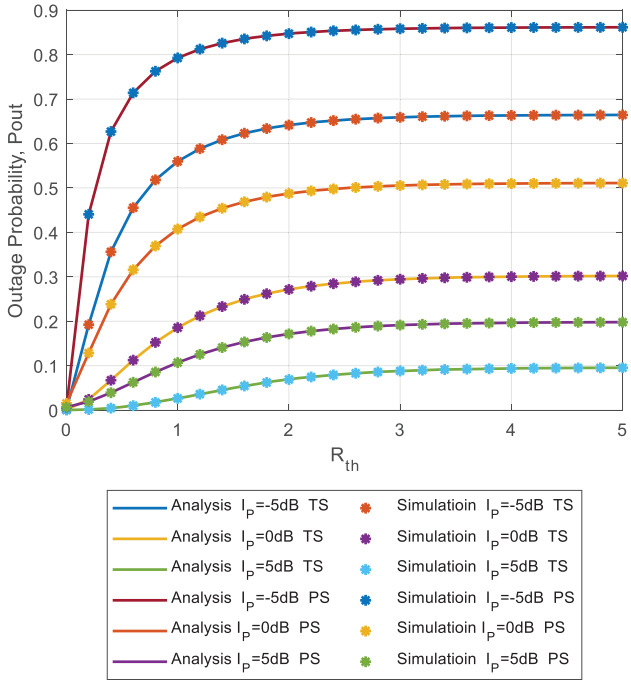

Figure 3: The curves of outage probability with different I_P and energy harvesting scheme

Fig. 4 simulates the outage probability as a function of the primary user's peak interference power I_p under different outage thresholds γ_{th} and various energy harvesting schemes. The simulation results indicate that the derived results of the proposed scheme match well with the Monte Carlo simulation results. As I_p gradually increases, the system computation offloading outage probability progressively diminishes and approaches zero. As the outage threshold γ_{th} continues to decrease, the system outage probability continues to decrease, that is, the less likely the system computation offloading is to be interrupted, and similarly, the system performance using TS energy harvesting scheme is superior to that of the PS energy harvesting scheme.

Fig. 5 simulates the outage probability as a function of the outage threshold γ_{th} under different primary user peak interference power I_P and various energy harvesting schemes. Simulation results reveal that the computation offloading outage probability increases with the increase of outage threshold γ_{th}. Similarly, under the same energy harvesting scheme and the same outage threshold, larger I_P means higher signal-to-noise ratio, which can compensate for the performance loss under harsh conditions.

Fig. 6 simulates the outage probability as a function of the number of relays under different primary user peak interference power I_p and various energy harvesting schemes. Under the condition of high I_P, the system outage probability is small, and as the number of relays K continues to increase, the system computation offloading outage probability continues to decrease. This is because the larger the value of K, the larger the range of UAV sets and the greater the probability that the performance of the optimal UAV selected from a large UAV set will be better than that of the optimal UAV selected from a small UAV set.

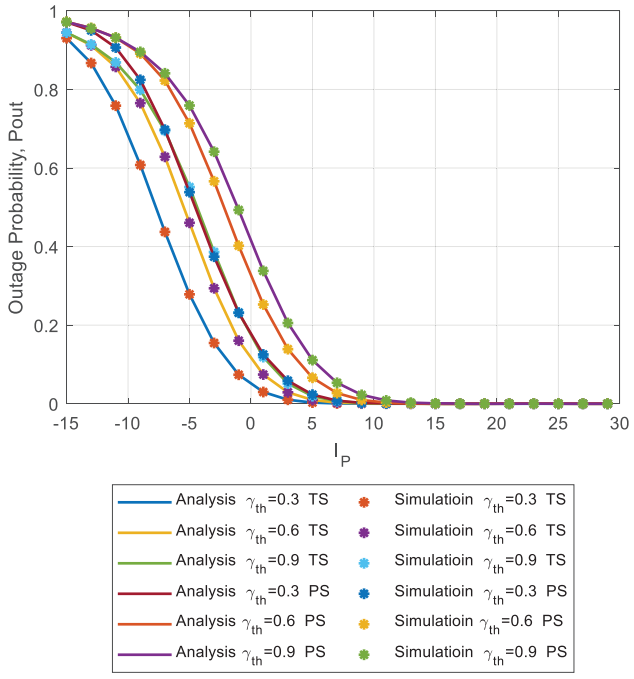

Figure 4: The curves of outage probability with different γ_{th} and energy harvesting scheme

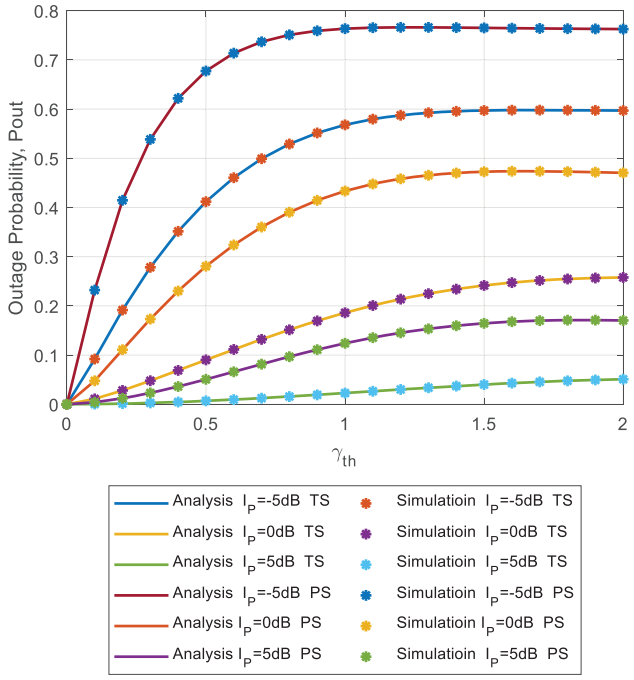

Figure 5: The curves of outage probability with different γ_{th} and energy harvesting scheme

Fig. 7 simulates the change of the outage probability curve with the primary user peak interference power I_p under different IRS elements and various energy harvesting schemes. At $N = 8$, the

probability of the system outage is lower than that of $N = 5$ and $N = 2$. This is because a larger number of IRS elements can improve the diversity gain of the system, thereby achieving better performance.

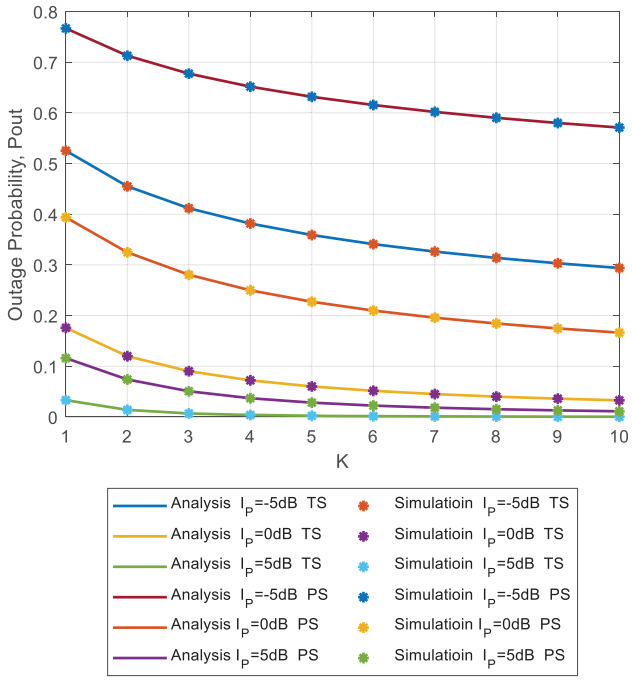

Figure 6: The curves of outage probability with different K and energy harvesting scheme

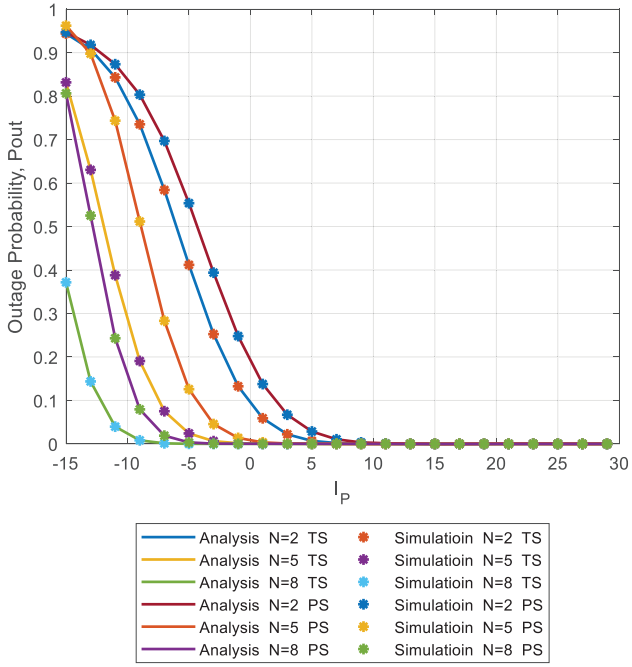

Figure 7: The curves of outage probability with different I_P and energy harvesting scheme

Fig. 8 simulates the change of the outage probability curve with time conversion factor ρ and power division factor η under different I_p. As I_p continues to increase, the constraints on user and UAV transmission power decrease, the system achieves a lower computation offloading outage probability. Moreover, the system outage probability tends to decrease slowly with the increase of the time conversion factor ρ; however, the decrease is not significant. The system outage probability gradually increases with the increase of the power division factor η, which indicates that the source node uses a larger proportion of power to harvest energy, i.e., if the power of the transmitted signal is smaller it results in a weaker signal received by the MEC server, therefore, the probability of system interruption increases.

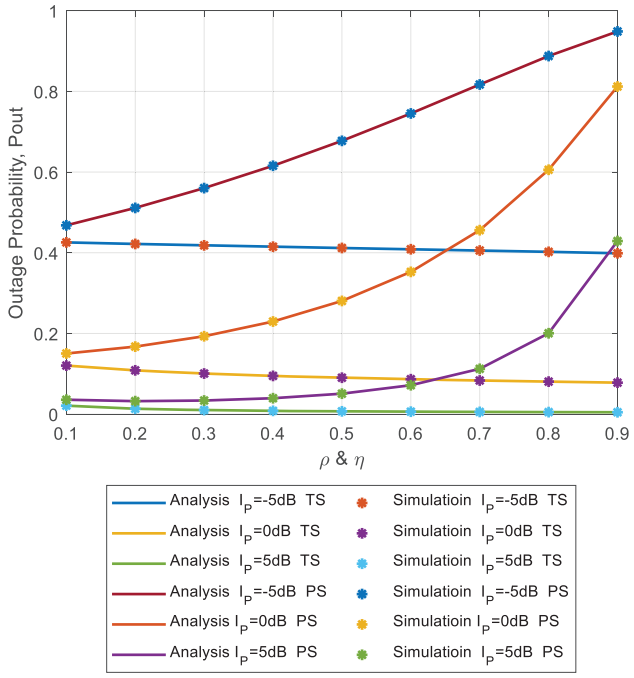

Figure 8: The curves of outage probability with different ρ/η and energy harvesting scheme

Fig. 9 simulates the change of outage probability curve *vs.* energy conversion coefficient ξ under different primary user peak interference power I_p and various energy harvesting schemes. The simulation results again verify the conclusion that the system computation offloading outage probability continues to decrease as I_p increases. Moreover, while the system computation offloading outage probability has a slow decreasing trend with the increase of energy conversion coefficient, the decrease is not significant.

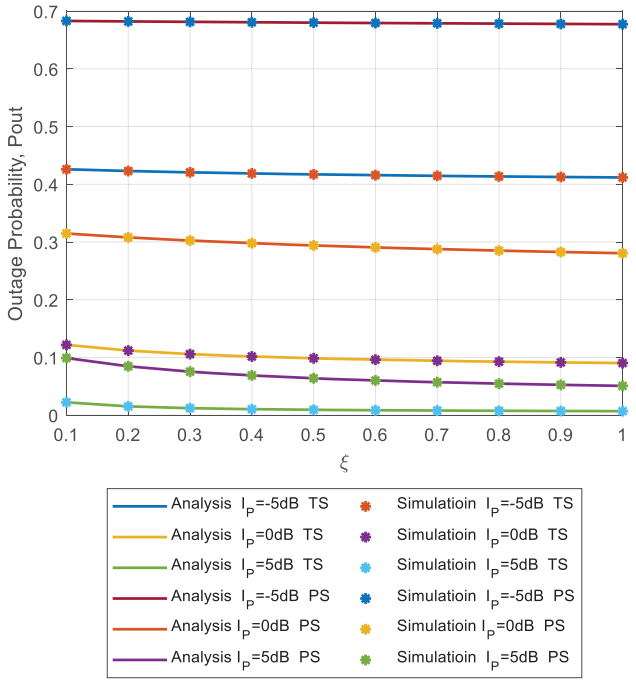

Figure 9: The curves of outage probability with different ξ and energy harvesting scheme

Fig. 10 simulates and compares the only optimal UAV transmission link, the only IRS transmission link, and the optimal UAV cooperative IRS system proposed in this paper. The simulation has been carried out under different energy harvesting schemes, when the outage probability varies with I_p. The simulation results show that under the same energy harvesting scheme, the optimal UAV cooperative IRS system proposed in this paper has a smaller outage probability than two traditional transmission links. This finding also verifies the effectiveness of the system model proposed in this article. When I_P is at a smaller value, the outage probability of the only optimal UAV transmission system using the TS energy harvesting scheme is superior to the optimal UAV cooperative IRS system using the PS energy harvesting scheme. This is because when the I_P value is smaller, the transmission power of the source node is extremely small under constraints, resulting in smaller power value used by the UAV to harvest energy. At this level, the outage probability of the UAV link inevitably increases, resulting in an increase in the computation offloading outage probability of the entire system, thus, verifying the conclusion that TS is superior to PS energy harvesting scheme. When I_P ranges between -5 and 0, the performance of the optimal UAV cooperative IRS system using the PS energy harvesting scheme begins to surpass that of the optimal UAV transmission only system using the TS energy harvesting scheme.

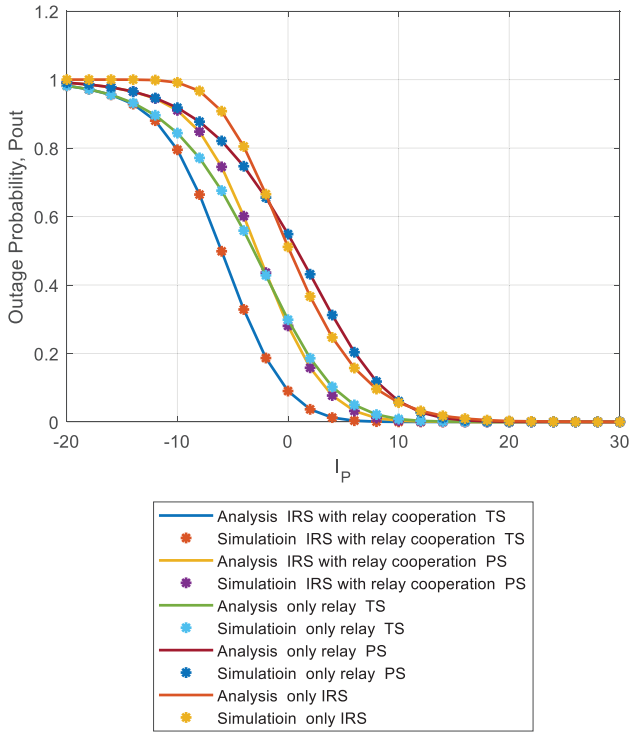

Figure 10: The curves of outage probability with different link and energy harvesting schemes

5 Conclusion

This paper presents an analysis of the outage probability of a Rayleigh fading channel-based energy harvesting enhanced optimal UAV cooperative IRS to assist users in offloading computing tasks to MEC servers' system model. The simulation results demonstrate that the theoretical analysis matches well with the actual simulation results, thereby validating the accuracy of the theoretical analysis presented in this paper. In addition, the proposed system is compared to a system that solely relies on optimal UAV link transmission and another system that exclusively relies on IRS link transmission. The simulation results indicate that the optimal UAV cooperative IRS system model proposed in this paper exhibits a higher computation offloading success rate. Due to the cluster communication characteristics of future mobile networks, in the face of massive computing tasks, in order to be closer to the actual situation, more complex heterogeneous and complex models will be considered, and AI and blockchain technology will be combined to optimize the computing offload performance.

Acknowledgement: Many thanks for the resources and materials provided by Henan University of Science and Technology and Henan Longmen Laboratory, and thank the team members for their support.

Funding Statement: This work was supported by the National Natural Science Foundation of China (62271192); Henan Provincial Scientists Studio (GZS2022015), Central Plains Talents Plan (ZYY-CYU202012173); National Key R&D Program of China (2020YFB2008400); the Program of CEMEE (2022Z00202B); LAGEO of Chinese Academy of Sciences (LAGEO-2019-2); Program for Science

& Technology Innovation Talents in the University of Henan Province (20HASTIT022); Natural Science Foundation of Henan under Grant 202300410126; Program for Innovative Research Team in University of Henan Province (21IRTSTHN015); Equipment Pre-Research Joint Research Program of Ministry of Education (8091B032129); Training Program for Young Scholar of Henan Province for Colleges and Universities (2020GGJS172); Program for Science & Technology Innovation Talents in Universities of Henan Province under Grand (22HASTIT020) and Henan Province Science Fund for Distinguished Young Scholars (222300420006).

Author Contributions: The authors confirm contribution to the paper as follows: study conception and design, formula derivation, analysis and interpretation of results: Baofeng Ji, Ying Wang; data collection, draft manuscript preparation: Weixing Wang; paper format review and language polishing: Shahid Mumtaz, Charalampos Tsimenidis. All authors reviewed the results and approved the final version of the manuscript.

Availability of Data and Materials: Due to team policies and confidentiality agreements, we cannot provide data. We have fully described the process of experimental design, analysis and results, as well as data analysis and processing.

Conflicts of Interest: The authors declare that they have no conflicts of interest to report regarding the present study.

References

1. Mohsan, S. A. H., Othman, N. Q. H., Mohamed, A. F. A., Mazinani, A., Amjad, H. (2021). A vision of 6G: Technology trends, potential applications, challenges and future roadmap. *International Journal of Computer Applications in Technology, 67(2–3),* 275–288.
2. Guo, F., Yu, F. R., Zhang, H., Li, X., Ji, H. et al. (2021). Enabling massive IoT toward 6G: A comprehensive survey. *IEEE Internet of Things Journal, 8(15),* 11891–11915.
3. Sanusi, J., Oshiga, O., Thomas, S., Idris, S., Adeshina, S. et al. (2021). A review on 6G wireless communication systems: Localization and sensing. *2021 1st International Conference on Multidisciplinary Engineering and Applied Science (ICMEAS)*, pp. 1–5. Abuja, Nigeria.
4. Zhou, F., Hu, R. Q., Li, Z., Wang, Y. (2020). Mobile edge computing in unmanned aerial vehicle networks. *IEEE Wireless Communications, 27(1),* 140–146.
5. Zhou, F., Wu, Y., Hu, R. Q., Qian, Y. (2018). Computation rate maximization in UAV-enabled wireless-powered mobile-edge computing systems. *IEEE Journal on Selected Areas in Communications, 36(9),* 1927–1941.
6. Wang, H., Ke, H., Sun, W. (2020). Unmanned-aerial-vehicle-assisted computation offloading for mobile edge computing based on deep reinforcement learning. *IEEE Access, 8,* 180784–180798.
7. Xu, H., Huang, W., Zhou, Y., Yang, D., Li, M. et al. (2021). Edge computing resource allocation for unmanned aerial vehicle assisted mobile network with blockchain applications. *IEEE Transactions on Wireless Communications, 20(5),* 3107–3121.
8. Ren, Y., Xie, Z., Ding, Z., Sun, X., Xia, J. et al. (2021). Computation offloading game in multiple unmanned aerial vehicle-enabled mobile edge computing networks. *IET Communications, 15(10),* 1392–1401.
9. Lin, C., Han, G., Shah, S. B. H., Zou, Y., Gou, L. (2021). Integrating mobile edge computing into unmanned aerial vehicle networks: An sdn-enabled architecture. *IEEE Internet of Things Magazine, 4(4),* 18–23.
10. Chen, R., Liu, M., Hui, Y., Cheng, N., Li, J. (2022). Reconfigurable intelligent surfaces for 6G IoT wireless positioning: A contemporary survey. *IEEE Internet of Things Journal, 9(23),* 23570–23582.

11. Huang, C., Zappone, A., Alexandropoulos, G. C., Debbah, M., Yuen, C. (2019). Reconfigurable intelligent surfaces for energy efficiency in wireless communication. *IEEE Transactions on Wireless Communications, 18(8),* 4157–4170.
12. Wu, Q., Zhang, R. (2020). Towards smart and reconfigurable environment: Intelligent reflecting surface aided wireless network. *IEEE Communications Magazine, 58(1),* 106–112.
13. Björnson, E., Özdogan, Ö., Larsson, E. G. (2020). Intelligent reflecting surface versus decode-and-forward: How large surfaces are needed to beat relaying? *IEEE Wireless Communications Letters, 9(2),* 244–248.
14. Madrid, M. B., Famaey, J., Lemic, F. (2022). Intelligent reflective surface vs. mobile relay-supported NLoS avoidance in indoor mmWave networks. *GLOBECOM 2022—2022 IEEE Global Communications Conference*, pp. 934–939. Rio de Janeiro, Brazil.
15. Liaskos, C., Tsioliaridou, A., Pitsillides, A., Ioannidis, S., Akyildiz, I. (2018). Using any surface to realize a new paradigm for wireless communications. *Communications of the ACM, 61(11),* 30–33.
16. Yan, W., Yuan, X., He, Z. Q., Kuai, X. (2020). Passive beamforming and information transfer design for reconfigurable intelligent surfaces aided multiuser MIMO systems. *IEEE Journal on Selected Areas in Communications, 38(8),* 1793–1808.
17. Dong, L., Wang, H. M. (2020). Enhancing secure MIMO transmission via intelligent reflecting surface. *IEEE Transactions on Wireless Communications, 19(11),* 7543–7556.
18. Hong, S., Pan, C., Ren, H., Wang, K., Nallanathan, A. (2020). Artificial-noise-aided secure MIMO wireless communications via intelligent reflecting surface. *IEEE Transactions on Communications, 68(12),* 7851–7866.
19. Zhi, K., Pan, C., Ren, H., Wang, K. (2021). Statistical CSI-based design for reconfigurable intelligent surface-aided massive MIMO systems with direct links. *IEEE Wireless Communications Letters, 10(5),* 1128–1132.
20. Bai, T., Pan, C., Deng, Y., Elkashlan, M., Nallanathan, A. et al. (2020). Latency minimization for intelligent reflecting surface aided mobile edge computing. *IEEE Journal on Selected Areas in Communications, 38(11),* 2666–2682.
21. Shafique, T., Tabassum, H., Hossain, E. (2021). Optimization of wireless relaying with flexible UAV-borne reflecting surfaces. *IEEE Transactions on Communications, 69(1),* 309–325.
22. Li, S., Duo, B., Yuan, X., Liang, Y. C., Di Renzo, M. (2020). Reconfigurable intelligent surface assisted UAV communication: Joint trajectory design and passive beamforming. *IEEE Wireless Communications Letters, 9(5),* 716–720.
23. Shen, H., Xu, W., Gong, S., He, Z., Zhao, C. (2019). Secrecy rate maximization for intelligent reflecting surface assisted multi-antenna communications. *IEEE Communications Letters, 23(9),* 1488–1492.
24. Cui, M., Zhang, G., Zhang, R. (2019). Secure wireless communication via intelligent reflecting surface. *IEEE Wireless Communications Letters, 8(5),* 1410–1414.
25. Lv, L., Wu, Q., Li, Z., Al-Dhahir, N., Chen, J. (2021). Secure two-way communications via intelligent reflecting surfaces. *IEEE Communications Letters, 25(3),* 744–748.
26. Wu, C., Yan, S., Zhou, X., Chen, R., Sun, J. (2021). Intelligent reflecting surface (IRS)-aided covert communication with warden's statistical CSI. *IEEE Wireless Communications Letters, 10(7),* 1449–1453.
27. Zhou, G., Pan, C., Ren, H., Wang, K., Nallanathan, A. (2020). A framework of robust transmission design for IRS-Aided MISO communications with imperfect cascaded channels. *IEEE Transactions on Signal Processing, 68,* 5092–5106.
28. Zargari, S., Khalili, A., Zhang, R. (2021). Energy efficiency maximization via joint active and passive beamforming design for multiuser MISO IRS-aided SWIPT. *IEEE Wireless Communications Letters, 10(3),* 557–561.

29. Zargari, S., Farahmand, S., Abolhassani, B., Tellambura, C. (2021). Robust active and passive beamformer design for IRS-aided downlink MISO PS-SWIPT with a nonlinear energy harvesting model. *IEEE Transactions on Green Communications and Networking, 5(4),* 2027–2041.
30. Liu, J., Xiong, K., Lu, Y., Ng, D. W. K., Zhong, Z. et al. (2020). Energy efficiency in secure IRS-aided SWIPT. *IEEE Wireless Communications Letters, 9(11),* 1884–1888.
31. Wu, Q., Zhang, R. (2020). Joint active and passive beamforming optimization for intelligent reflecting surface assisted SWIPT under QoS constraints. *IEEE Journal on Selected Areas in Communications, 38(8),* 1735–1748.
32. Li, Z., Chen, W., Wu, Q., Wang, K., Li, J. (2022). Joint beamforming design and power splitting optimization in IRS-assisted SWIPT NOMA networks. *IEEE Transactions on Wireless Communications, 21(3),* 2019–2033.
33. Khalili, A., Zargari, S., Wu, Q., Ng, D. W. K., Zhang, R. (2021). Multi-objective resource allocation for IRS-aided SWIPT. *IEEE Wireless Communications Letters, 10(6),* 1324–1328.
34. Xu, D., Yu, X., Jamali, V., Ng, D. W. K., Schober, R. (2021). Resource allocation for large IRS-assisted SWIPT systems with non-linear energy harvesting model. *2021 IEEE Wireless Communications and Networking Conference (WCNC)*, pp. 1–7. Nanjing, China.
35. Wu, Q., Zhang, R. (2020). Weighted sum power maximization for intelligent reflecting surface aided SWIPT. *IEEE Wireless Communications Letters, 9(5),* 586–590.
36. Fu, M., Zhou, Y., Shi, Y., Letaief, K. B. (2021). Reconfigurable Intelligent surface empowered downlink non-orthogonal multiple access. *IEEE Transactions on Communications, 69(6),* 3802–3817.
37. Zheng, B., Wu, Q., Zhang, R. (2020). Intelligent reflecting surface-assisted multiple access with user pairing: NOMA or OMA? *IEEE Communications Letters, 24(4),* 753–757.
38. Abdullah, Z., Chen, G., Lambotharan, S., Chambers, J. A. (2020). A hybrid relay and intelligent reflecting surface network and its ergodic performance analysis. *IEEE Wireless Communications Letters, 9(10),* 1653–1657.
39. Zou, Y., Wang, X., Shen, W. (2013). Optimal relay selection for physical-layer security in cooperative wireless networks. *IEEE Journal on Selected Areas in Communications, 31(10),* 2099–2111.
40. Ji, B., Huang, J., Wang, Y., Song, K., Li, C. et al. (2023). Multi-relay cognitive network with anti-fragile relay communication for intelligent transportation system under aggregated interference. *IEEE Transactions on Intelligent Transportation Systems, 24(7),* 7736–7745.
41. Yang, L., Meng, F., Wu, Q., da Costa, D. B., Alouini, M. S. (2020). Accurate closed-form approximations to channel distributions of RIS-aided wireless systems. *IEEE Wireless Communications Letters, 9(11),* 1985–1989.
42. Peppas, K. P. (2011). Accurate closed-form approximations to generalised-K sum distributions and applications in the performance analysis of equal-gain combining receivers. *IET Communications, 5(7),* 982–989.